ARTICLES

Electron Paramagnetic Resonance Study of the Dynamics of H and D Atoms Trapped in Substituted Silasesquioxane Cages

Barbara Gross,[†] Herbert Dilger,[†] Robert Scheuermann,[†] Michael Päch,[‡] and Emil Roduner*[,†]

Institute of Physical Chemistry, University of Stuttgart, Pfaffenwaldring 55, 70569 Stuttgart, Germany, and Radiation Laboratory, University of Notre Dame, Notre Dame, Indiana 46556

Received: June 12, 2001; In Final Form: August 23, 2001

The hyperfine coupling (hfc) constants, *A*, and the *g*-factors of hydrogen isotopes confined in silasesquioxane ($R_8Si_8O_{12}$) cages show significant deviations from the free-particle vacuum value thus revealing the influence of the environment on the wave function of the trapped atom. Accurate measurements of the hfc constants in the temperature range of 5−300 K show a strong isotope effect, different substituents on the cage corners having a clear influence on both static and dynamic cage effects. Deviations of *g*-factors from the free-electron value are independent of temperature, but they depend on substituents. To gain information about the factors influencing the trapped atoms' dynamic behavior inside the cage environments, a phenomenological model developed previously for the description of the dynamics of hydrogen isotopes in liquid water and ice (*J. Chem. Phys.* **1995**, *102*, 5989), which is based on the spherical harmonic oscillator, is applied to the more rigid silasesquioxane cage systems. The present study aims at a better understanding of matrix effects on the dynamics of particles in a constraining environment, a problem which represents a challenge for both phenomenological modeling and quantum chemical calculations.

1. Introduction

In 1994, Sasamori and co-workers found that silasesquioxanes are able to stabilize radiolytically generated hydrogen atoms inside their cavities.[1] These trapped radicals were shown to be remarkably long-lived at room temperature, even in solution and in the presence of oxygen or other radical scavengers.

Since then, these systems have been subject to various experimental and theoretical investigations.[2] Päch and Stösser[3] investigated the trapping and detrapping mechanisms and the influence of radical scavengers present during irradiation of the compounds. They showed that intramolecular processes participate in the trapping process and could also give an explanation for satellite signals observed in the electron paramagnetic resonance (EPR) spectra. Their experimentally determined activation and reaction energies are in good agreement with recent theoretical results obtained by Mattori and co-workers,[4] who in addition presented vibrational frequencies for the octahydridosilasesquioxane (HT_8) and for trapped H ($H@HT_8$) and calculated values for the isotropic hyperfine coupling (hfc) constant of trapped hydrogen in HT_8 using different ab initio methods. Comparison of the calculated frequencies to an experimental study of HT_8 in CCl_4 by Bürgy et al.[5] showed them to be in satisfying agreement.

Another point of interest in these and similar systems is the question of how the encaged atoms behave inside their confining environments. Adrian[6] worked out the coupling effects of the van der Waals interaction, which reduces the hyperfine coupling of the trapped hydrogen by diluting its wave function at the nucleus, and the Pauli exclusion forces, which are of shorter range and serve to increase the hyperfine coupling of the trapped atom. While this was for a static atom, Dmitriev and Zhitnikov[7] extended the model by including the effect of zero-point vibrational motion to accommodate isotope effects. Spaeth[8] used a similar model to analyze EPR, electron nuclear double resonance (ENDOR), and muon spin resonance, μSR (in a chemical sense, muonium ($Mu = \mu^+e^-$), behaves like a hydrogen isotope with a mass of one-ninth of the mass of ^1H) studies on hydrogen isotopes in alkali halides. The work provided evidence for the existence of several different trapping sites in alkali halide solids, as well as for the dynamic behavior of the trapped species. Spaeth showed that, in the case of hydrogen and deuterium atoms in alkali halides, the dynamics is described in a good approximation by localized vibrations in a static lattice. Prassides et al.[9] investigated endohedral muonium in C_{70} and proved experimentally the nonspherical charge distribution inside the cage due to the nonspherical shape of the cage. These results were supported by a theoretical study by Claxton.[10] Dynamic behavior of hydrogen isotopes in liquid water and ice was studied by means of EPR and μSR, and the results were interpreted in terms of a phenomenological model based on the three-dimensional harmonic oscillator.[11] This was the first work that accounted for a temperature dependence of the hyperfine coupling.

Previous temperature-dependent EPR studies on hydrogen isotopes encaged in the octaethyl- and octa(trimethylsiloxy)-silasesquioxanes, EtT_8 and Q_8M_8,[12] were already interpreted in

* To whom correspondence should be addressed. E-mail: E.Roduner@ipc.uni-stuttgart.de.
[†] University of Stuttgart.
[‡] University of Notre Dame.

10.1021/jp012220k CCC: $20.00
Published on Web 10/11/2001

terms of the abovementioned model. We now present a more detailed EPR investigation on hydrogen and deuterium atoms in these cage systems, extending the temperature range down to 5 K, and on atomic hydrogen in two further cage derivatives, the octamethyl- and octahydridosilasesquioxanes, MeT_8 and HT_8. Measuring the temperature dependence of the hyperfine coupling constant and the *g*-factor of hydrogen and deuterium inside different cage environments should lead to a better understanding of cage effects on the dynamics, including the influence of substituents, and allow us to check the validity of the simple oscillator model.

2. Phenomenological Model

Because the hfc constant is directly proportional to the electron spin density at the nucleus, i.e., $|\Psi(0)|^2$, a model must provide a description for the influence of the environment on the wave function of the atom at the nucleus. The model by Roduner et al.[11] separates compression and delocalization effects, influencing the wave function of a static atom in the cage center, from dynamic contributions brought about by the vibration of the atom in the cavity. Applying this model to silasesquioxane cages, we neglect vibrational coupling between the atom's vibrational modes and those of the cage framework.

Static effects include the compression of the wave function due to Pauli exclusion forces on one hand, leading to an increased hyperfine interaction, and van der Waals interaction leading to spin delocalization onto neighboring cage atoms on the other hand, producing a decrease of the hfc constant, *A*, relative to its value in a vacuum, A_{vac}. Dynamic contributions are due to the dependence of spin delocalization on the distance between the vibrating trapped atom and the surrounding cage and to the admixing of excited functions with nonspherical symmetry to the ground-state 1s wave function brought about by the distortion when the atom collides with the cage. Both effects will result in a decrease of the hyperfine interaction with rising temperature.

The ratio $f = A/A_{vac}$ is written as an expansion in terms of a displacement coordinate *Q*, in which odd powers in *Q* average to zero for spherical symmetry, which is a reasonable assumption for sufficiently fast oscillation of the trapped atom to average out a dynamic deformation of the vibrational potential. For a vibrational state, v, we have

$$\langle f\rangle_v = \langle A\rangle_v/A_{vac} = 1 + c_0 + c_2\langle Q^2\rangle_v + c_4\langle Q^4\rangle_v + \ldots \quad (1)$$

In the approximation of a spherical isotropic harmonic oscillator, the expansion is truncated, retaining only the quadratic term in *Q*, and we write

$$\langle Q^2\rangle_v = \langle X^2\rangle_{v_x} + \langle Y^2\rangle_{v_y} + \langle Z^2\rangle_{v_z} = \langle R^2\rangle_{v_x,v_y,v_z} \quad (2)$$

with the mean square displacement from the cage center given by

$$\langle R^2\rangle_{v_x,v_y,v_z} = \frac{h\nu}{k}\left(\frac{3}{2} + \upsilon_x + \upsilon_y + \upsilon_z\right) \quad (3)$$

Here, ν is the vibrational frequency, *k* is the force constant, and υ_x, υ_y, and υ_z are the vibrational quantum numbers of the three-dimensional oscillator.

It must be kept in mind that there is no fundamental justification for the harmonic approximation. The potential could well have a relatively flat base or even a slight maximum at the center of the cage. The harmonic approximation seems to be appropriate for H atoms in a C_{60} cage, but for C_{70}, a double minimum along the long axis was predicted from ab initio calculations.[10]

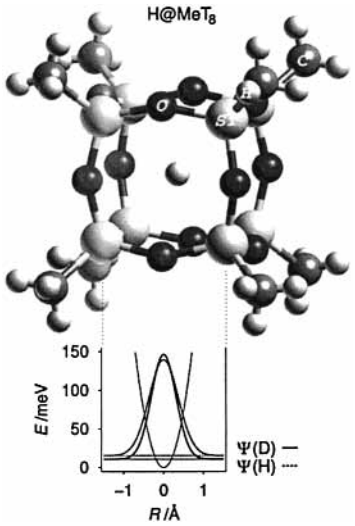

Figure 1. Structure of the octamethylsilasesquioxane molecule with the trapped H isotopes and their zero-point vibrational wave functions. Atoms are drawn with one-fourth of their tabulated van der Waals radii.

In the simplest approach, the dynamic contributions are assumed to scale linearly with the mean square displacement of the trapped atom. However, this dependence is almost certainly more complex, as has already been postulated by Adrian,[6] and it is expected to vary more with cage substitution than the potential. In the linear approach, the ratio *f* at zero temperature is expressed as

$$\langle f\rangle_0 = A/A_{vac} = 1 + c_0 + \frac{3}{2}c_2\beta \quad (4)$$

Here, c_0 is an experimental parameter including the mentioned static contributions, and the term $^3/_2c_2\beta$ describes the contribution of the zero point vibration. A_{vac} was reported to amount to 1420.405 752 MHz for hydrogen[13] and 218.256 235 MHz for deuterium.[14] The temperature dependence of *f* is then obtained from the Boltzmann average over all thermally excited vibrational states:

$$\langle f\rangle(T) = 1 + c_0 + c_2\beta\frac{\sum_{\upsilon_x,\upsilon_y,\upsilon_z}\left(\frac{3}{2} + \upsilon_x + \upsilon_y + \upsilon_z\right)\exp\left[-(\upsilon_x + \upsilon_y + \upsilon_z)\frac{h\nu}{k_BT}\right]}{\sum_{\upsilon_x,\upsilon_y,\upsilon_z}\exp\left[-(\upsilon_x + \upsilon_y + \upsilon_z)\frac{h\nu}{k_BT}\right]} \quad (5)$$

While ν, and hence $\beta = h\nu/k$, are related to *k* via $2\pi\nu = \sqrt{k/m}$ and therefore depend on the isotope mass, *k* itself (assuming simple scaling of ν with $m^{-1/2}$), c_0, and c_2 are free parameters. Within a given cage system, these parameters should consequently have the same values, independent of the mass of the encaged isotope.

Figure 1 shows the molecular structure of one of the investigated systems, the octamethylsilasesquioxane with a trapped hydrogen atom (H@MeT_8). The ball size in the illustration corresponds to $^1/_4$ of the tabulated van der Waals radii of the cage atoms.[15] The potential energy and the H and D zero-point energies were calculated using the experimentally determined force constant *k*. The corresponding wave functions for the vibrational ground state are shown on a relative scale.

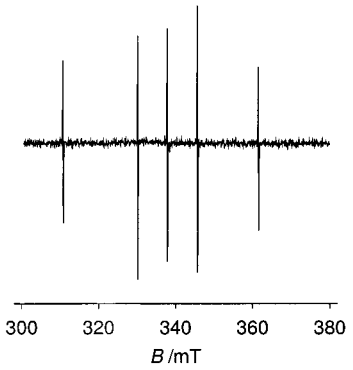

Figure 2. X-band EPR spectra of H/D@Q_8M_8 at 293 K. The outer two lines belong to H, the three center lines to D atoms.

3. Experimental Section

The hfc constants of hydrogen inside Q_8M_8, EtT_8, MeT_8, and HT_8 and of deuterium inside Q_8M_8 and EtT_8 were measured in the temperature range from 5 K to room temperature using a Bruker EMX X-band EPR spectrometer equipped with an Oxford continuous flow helium cryostat ESR 900. To minimize saturation effects due to the very slow relaxation times at low temperatures, the microwave power was continually decreased with temperature down to 200 nW. The magnetic field was calibrated at ambient temperature using an in-cavity NMR probe.

The silasesquioxane derivatives were synthesized as described in ref 3 and subsequently γ-irradiated in air with a dose of 110 kGy using a ^{60}Co source at Willy Rüsch AG, Kernen, Germany, to generate atoms in the cages. The powder samples were sealed in quarz tubes under a pressure of 100 mbar He at room temperature.

Figure 2 shows the complete EPR spectra of H/D@Q_8M_8, a sample containing both hydrogen and deuterium atoms enclosed in (nondeuterated) Q_8M_8 cages, which is achieved by performing the γ-irradiation in solution in the presence of deuterated solvents. To obtain the hfc constants with the required accuracy, each of the resonances was recorded separately, the exact positions being determined to 10^{-3} mT by fitting Gaussian functions to the experimental data using the MINUIT fitting algorithms.[16]

At the lowest temperatures, below ca. 40 K, the lines are significantly distorted and also shifted depending on the sweep direction. This is mostly due to the very long electron T_1 relaxation which leads to passage-dependent saturation effects. Because the shifts are similar for all lines, this does not influence the hfc but still leads to large errors. It was verified that these points do not significantly perturb the fits of $f(T)$. The effect would be fatal, however, for the determination of g, and points below 40 K are therefore omitted in the discussion of g.

Because second-order perturbation theory is not sufficiently accurate for the analysis of small temperature effects, the hfc constants and g-factors were calculated analytically from the EPR transition frequencies and resonance fields. The corresponding systems of equations[17] were solved with the aid of the MAPLE software package.[18]

The force constant k and the parameters c_0 and c_2 were determined by fitting eq 5 to the experimental data sets using, again, the MINUIT program library.

Previous experimental results[12] are in good agreement with the data presented here; therefore, they are included in this work and marked with filled symbols in Figures 3 and 5. Also, we use results of previously published μSR experiments on muonium in EtT_8 for comparison of isotope effects in Figure 6.[12]

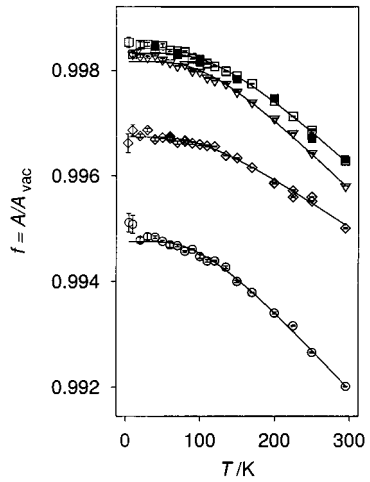

Figure 3. Temperature dependence of the hydrogen atom hfc constant in differently substituted silasesquioxanes: H@Q_8M_8 (□/■), H@EtT_8 (◇), H@HT_8 (⊙), H@MeT_8 (▽).

4. Results and Discussion

A. Temperature and Substitution Dependence of the Hyperfine Coupling of Trapped H and D Atoms. Figure 3 shows the relative hfc constants, f, of hydrogen in four different cage environments as a function of temperature together with the functions obtained by fitting eq 5 to each of the experimental data sets. It is obvious that different substituents on the cage corners have a clear impact on the hyperfine interaction of trapped hydrogen atoms, as well as on its temperature behavior. While the couplings are always below the vacuum value, the four curves are significantly displaced from each other, and H@EtT_8 displays a temperature dependence with a significantly smaller slope.

The constant c_0, describing the combined static influences on the wave function at the cage center, and the contribution of zero-point vibration ($^3/_2(c_2\beta)$) determine the intercept of the curve at zero temperature. From eq 5, we expect a plateau value in the low-temperature region up to the point where higher vibrational modes are thermally excited. This point is crucially dependent on the potential energy, in terms of the applied model represented by the force constant, the slope being determined by the parameter c_2. Figure 3 reveals that the temperature behavior of the hfc constants found experimentally is well-reproduced by eq 5, showing the assumptions made to be qualitatively reasonable. Furthermore, we see immediately that different cage substitution does not merely alter the static contributions but that it also affects the slope of the curve at higher temperature. This reveals that the magnitude of the influence of dynamics depends on the nature of the organic substituent. Table 1 contains the parameters obtained from the fits.

The values of k for different cage systems are quite similar. Within the limits of the model, we therefore conclude that the nature of the substituent does not alter the potential energy at the cage centers to a large extent. Structural data[19−22] reveal comparable cavity dimensions in the solid state, Q_8M_8 having the smallest cross section and the hydrogen and alkyl derivatives providing somewhat larger and among each other very similarly sized cavities. The average body diagonal of a cage varies from 5.33 to 5.39 Å for the present examples, most cages showing a minor distortion from cubic symmetry in the solid.[24] It is reasonable to obtain the largest force constant for the smallest cage molecule, but a further correlation between cage dimensions and the value of k cannot be established.

TABLE 1: Substituent Effects—Parameter Results from Single Fits of Eq 5 for Hydrogen in Different Cages

	H@HT_8	H@MeT_8	H@EtT_8	H@Q_8M_8
c_0	$-2.39(7) \times 10^{-3}$	$0.94(7) \times 10^{-3}$	$-1.52(4) \times 10^{-3}$	$1.3(1) \times 10^{-3}$
c_2, nm^{-2}	−0.66(3)	−0.69(3)	−0.39(1)	−0.83(6)
k, N m^{-1}	3.2(1)	3.7(1)	3.12(9)	4.6(2)
$\tilde{\nu}_0$, cm^{-1}	232	250	229	278
$(\langle R^2\rangle_{0,0,0})^{1/2}$, Å	0.46	0.45	0.47	0.42
$E_{0,0,0}$, kJ mol^{-1}	4.16	4.48	4.11	4.99
$(^3/_2)c_2\beta$	-1.43×10^{-3}	-1.39×10^{-3}	-0.85×10^{-3}	-1.50×10^{-3}
$\bar{g}(T = 50-300$ K)	2.003 06(1)	2.002 95(2)	2.002 94(2)	2.002 73(2)

c_0 is negative for the hydrido- and ethylsilasesquioxanes, whereas for the methyl- and trimethylsiloxy derivatives, we obtain positive values. A positive value of c_0 means that compression dominates; for a negative c_0, delocalization wins. The importance of the zero-point vibration can be assessed by comparison of the offsets of the experimental data from unity in the low-temperature regime in Figure 3 with the c_0 values in Table 1. While c_0 leads to both negative and positive deviations of A from A_{vac}, this is offset by the vibrational contribution, given by $^3/_2(c_2\beta)$, which is always negative.

Assuming that due to similar cage dimensions and potentials the static compression effect will also be similar in magnitude for the different cages, the variations of the parameter c_0 might be attributed to a different amount of spin delocalization for different substituents, but the picture is additionally complicated by the possible effect of spin polarization. While delocalization is thought to simply transfer positive spin density onto the cage, thereby reducing its value on the trapped hydrogen atom, spin polarization creates negative spin density on the cage and thus permits an enhancement on the trapped atom.

The amount of spin population on cage atoms is estimated from ^{29}Si superhyperfine couplings, which had been reported to be ca. 0.15 mT for alkyl substituted cages and a factor 2.5 less in the case of $OSi(CH_3)_3$ substitution.[3] Given that a full electron spin on Si leads to a coupling of 164 mT,[23] the spin population comes to ca. 0.09% per Si atom in alkyl substituted cages or a total of 0.7% for all eight Si atoms (0.3% in Q_8M_8). By comparison with Figure 3, one may argue that this accounts roughly for the missing spin population on the trapped hydrogen atom. However, the fact that both couplings decrease with temperature shows that things are more complicated; moreover, the spin population on the oxygen atoms is not known. The best presently available quantum chemical calculations on this system[4] do not report any spin populations on the cage, and with the best basis set, they predict a deviation from the vacuum value of the trapped atom that is about an order of magnitude larger than that found experimentally.

The frequencies of zero-point vibration ($\tilde{\nu}_0$), the zero-point energies ($E_{0,0,0} = {}^3/_2(h\nu_0)$), and the values for the root-mean-square (rms) displacement ($(\langle R^2\rangle_{0,0,0})^{1/2}$) given in Table 1 were calculated from the force constants (k). The values obtained for $\tilde{\nu}_0$ between 230 and 280 cm^{-1}, as well as the zero-point vibrational energy, ranging from 4.11 to 4.99 kJ mol^{-1}, agree with Roduner's results for hydrogen in water ($\tilde{\nu}_0 = 252$ cm^{-1} and $E = 4.5$ kJ mol^{-1} [11]) and for H in a Krypton matrix (265 cm^{-1} [7]). Within the limits of our model, this implies that there is not much difference between a water cage, a silasesquioxane cage, and a Krypton matrix confining a hydrogen isotope. Obviously, on the time scale of the H atom oscillation, the stiffness of a silasesquioxane cage with well-defined chemical bonds is similar to that of a hydrogen-bonded water cage in its aqueous environment. The rms displacement values give an impression of the spatial requirement of the enclosed wave package in its particular environment. They are below the Bohr radius, a_0, of the guest atom in all cases. Mattori et al. predict 418 cm^{-1} for $\tilde{\nu}_0$ of H@HT_8 (this mode is mislabeled as additional Si−O−Si bend in Table 2 of ref 4), a value which requires a force constant that is a factor of 3 higher than that deduced from the experimental data in Figure 3.

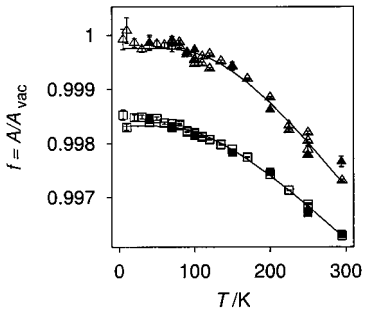

Figure 4. Temperature dependence of the hydrogen (□/■) and deuterium (△/▲) atom hfc constants in Q_8M_8.

As outlined above, the force constant and the parameters c_0 and c_2 are by definition mass-independent; therefore, they should adopt identical values for both hydrogen and deuterium isotopes trapped in identical cage environments. Figure 4 shows the experimental coupling constants for H and D in Q_8M_8 as a function of temperature, and the fit results obtained using eq 5.

While the qualitative aspect of the temperature dependence is still reproduced appropriately for both isotopes, the resulting parameters listed in Table 2 reveal significant differences between the two isotopes. The force constant for D in Q_8M_8 is extremely high, and its effect appears to be compensated partly by c_0 and c_2. Because in the case of Q_8M_8 the two data sets were obtained with the identical, partly deuterated sample, this has to be considered a distinct evidence for some deficiency in the model used here to describe the system.

With isotope-independent parameters c_0, c_2, and k, it should be possible to determine a single set of parameters valid for both isotopes by fitting eq 5 to both data sets simultaneously. Figure 5 shows the result of this so-called *global* fit for H and D in EtT_8, giving $k = 6.9$ N m^{-1}, $c_0 = 0.22 \times 10^{-3}$, and $c_2 = -1.21$ nm^{-2}. On the basis of these values, we calculated the corresponding function for the temperature behavior of the hyperfine coupling of muonium in EtT_8. While we obtain a force constant similar to the one obtained from individual fits, we see clearly that the global fit does not adequately represent the experimental data; in particular, it does not reproduce the data for Mu. The overall conclusion which has to be drawn from these observations is that the simple phenomenological model is obviously not appropriate to describe the dynamics of hydrogen isotopes in silasesquioxane cages with the desired accuracy.

Finally, we compare what the semiquantitative work by Adrian[6] would predict. The radius of a silasesquioxane cage is ca. $5.0a_0$. At this distance from the trapped atom, Adrian predicts for all noble gases (Ne, Ar, and Kr with a size that should be

TABLE 2: Isotope Effects—Parameter Results from Single and Global Fits of Eq 5 for Hydrogen and Deuterium in Q_8M_8 and EtT_8

	H@Q_8M_8	D@Q_8M_8	H/D@Q_8M_8	
c_0	$1.3(1) \times 10^{-3}$	$5.0(1) \times 10^{-3}$	$4.05(2) \times 10^{-3}$	
c_2, nm^{-2}	−0.83(6)	−3.5(2)	−2.29(1)	
k, N m^{-1}	4.6(2)	13.6(5)	9.22(3)	
$\tilde{\nu}_0$, cm^{-1}	278	339	394 (H)	279 (D)
$(\langle R^2\rangle_{0,0,0})^{1/2}$, Å	0.42	0.27	0.36 (H)	0.30 (D)
$E_{0,0,0}$, kJ mol^{-1}	4.99	6.07	7.07 (H)	5.00 (D)
$(^3/_2)c_2\beta$	-1.5×10^{-3}	-2.6×10^{-3}	-2.9×10^{-3} (H)	-2.1×10^{-3} (D)
$\bar{g}(T = 50-300$ K)	2.002 73(2)	2.002 73(2)		

	H@EtT_8	D@EtT_8	H/D@EtT_8	
c_0	$-1.52(4) \times 10^{-3}$	$-0.7(2) \times 10^{-3}$	$0.22(4) \times 10^{-3}$	
c_2, nm^{-2}	−0.39(1)	−0.4(2)	−1.21	
k, Nm^{-1}	3.12(9)	3(1)	6.90(8)	
$\tilde{\nu}_0$, cm^{-1}	229	159	341 (H)	241 (D)
$(\langle R^2\rangle_{0,0,0})^{1/2}$, Å	0.47	0.40	0.38 (H)	0.32 (D)
$E_{0,0,0}$, kJ mol^{-1}	4.11	2.85	6.11 (H)	4.32 (D)
$(^3/_2)c_2\beta$	-0.9×10^{-3}	-0.6×10^{-3}	-1.8×10^{-3} (H)	-1.3×10^{-3} (D)
$\bar{g}(T = 50-300$ K)	2.002 94(2)	2.002 96(1)		

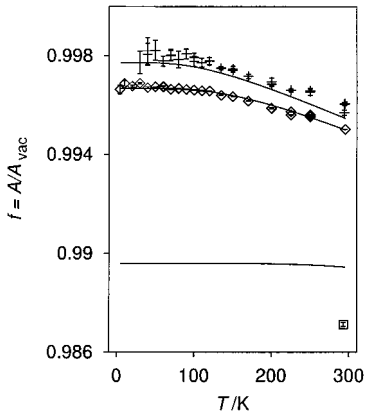

Figure 5. Global temperature dependence fit of the hydrogen (◇) and deuterium (+) atom hfc constants in EtT_8 and calculated function for muonium (□) in EtT_8.

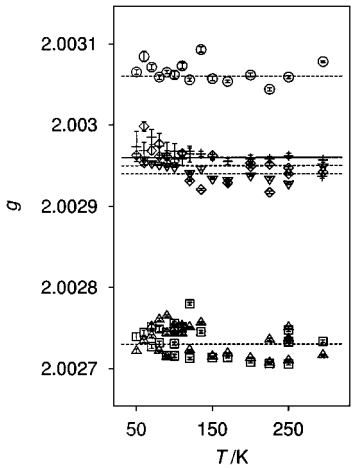

Figure 6. Temperature behavior of the g-factors in differently substituted silasesquioxane cages: H/D@Q_8M_8 (□/△), H/D@EtT_8 (◇/+), H@HT_8 (⊙), H@MeT_8 (▽). The lines give the average g-factors between 50 and 300 K.

comparable to that of the Si and O atoms) that the Pauli exclusion forces dominate the distance dependence of the hyperfine shift. This means that the lighter isotopes, which in the vibrational average spend more time near the cage wall, should be expected to have larger hyperfine shifts. Moreover, there should be a positive temperature dependence. Experimentally, both the mass and the temperature effects show the opposite behavior, thus indicating that in Adrian's model applied to silasesquioxanes the van der Waals forces should dominate the effect.

B. Matrix Effects on the *g*-Factor. Figure 6 shows the temperature behavior of the g-factors obtained for hydrogen and deuterium isotopes in different silasesquioxanes. Obviously, g-factors are not temperature-dependent but are clearly influenced by varying substitution at the cube corners. For hydrogen and deuterium isotopes in an identical environment, g-factors are in satisfying agreement, showing that the method of determination of resonance positions is sufficiently accurate.

For a free ^{1}H atom, the electronic g-factor is reported to be 2.002 284,[25] which is close to the free-electron value (g_e = 2.002 319[26]), whereas the g-factors found for the investigated silasesquioxane systems are across the board greater than g_e. These deviations from the free-electron value are due to spin−orbit coupling contributions; for hydrogen isotopes, we therefore have to presume the admixing of excited wave functions, because the 1s ground state has no angular momentum. According to Atherton,[27] admixing of excited hydrogen atom functions would lead to a decrease in g values; therefore, the positive g-factor shift must be produced by an interaction with the neighboring cage wave functions, which is equivalent to a partial transfer of spin density onto cage atoms or to spin polarization of the cage. This also provides an explanation for the dependence on cage substituents.

Investigations of Spaeth on hydrogen and muonium in alkali halides[8] showed a correlation between the deviations of hfc constants from the free atom's vacuum value and those of g-factors from the free-electron value. For negative deviations of A from A_{vac}, positive values for $\Delta g = g - g_e$ are found, and vice versa. This is in qualitative accordance with our results. The only theoretical treatment seems to be that of Adrian.[6] It can only accommodate negative values of Δg and is thus not suited to account for the positive shifts found in the present work.

It is striking that the largest shift is found for the lightest substituent (R = H), while R = alkyl gives intermediate values and R = trimethylsiloxy leads to the smallest shift. Obviously, the effect is not primarily related to the spin−orbit coefficients of substituent orbitals. It is more likely that substitution affects

the energetic ordering of cage molecular orbitals of suitable symmetry (angular momentum).

5. Conclusions

Temperature-dependent EPR measurements of the hfc constants of hydrogen atoms trapped inside different silasesquioxane cages show that cage effects on the wave function are influenced by the nature of the substituents. Because from the presented results we cannot derive a clear tendency, it remains difficult to attribute the observed deviations from the hfc constant in a vacuum to a single distinct effect.

The *g*-factors for the trapped species are larger than that of the free electron, revealing the existence of spin−orbit coupling contributions originating from partial spin delocalization onto cage atoms. The *g*-factors are not temperature-dependent but are influenced by substituents in the opposite way to hfc constants. As this inverse proportionality is only qualitative, we conclude that spin delocalization is an important factor but certainly not the sole environmental influence in these systems.

Comparison of temperature dependence of the hfc constants of trapped hydrogen and deuterium atoms reveals immediately their dynamic behavior inside the cage. While individual three-parameter fits of a harmonic oscillator model to the experimental data show that the description in terms of this model is qualitatively reasonable, there is insufficient consistency between parameters for different isotopes in identical cage environments, and there are significant deviations in fits with global parameters.

For a better description of the dynamics of the trapped atoms, we have to reconsider the approximations on which the phenomenological model is based. This model was reduced to three parameters because it was considered inappropriate to fit a more elaborate model to such simple experimental curves. The assumptions of a harmonic vibrational potential and of a linear dependence of spin delocalization on the H displacement coordinate have to be considered as a first step in developing a comprehensive model. The dynamic contributions are expected to vary even more strongly with cage substitution than the potential. For both problems, input from high-level ab initio calculations is called for. As for today, the calculation of reliable hyperfine couplings to the accuracy required here is still a formidable task, while relative potential energies should be accessible.

Acknowledgment. We thank the Willy Rüsch AG, Kernen i.R., Germany, for performing the γ-irradiations of our samples.

References and Notes

(1) Sasamori, R.; Okaue, Y.; Isobe, T.; Matsuda, Y. *Science* **1994**, *265*, 1691.
(2) Hayashino, Y.; Isobe, T.; Matsuda, Y. *Inorg. Chem.* **2001**, *40*, 2218.
(3) Päch, M.; Stösser, R. *J. Phys. Chem. A* **1997**, *101*, 8360.
(4) Mattori, M.; Mogi, K.; Sakai, Y.; Isobe, T. *J. Phys. Chem. A* **2000**, *104*, 10868.
(5) Bürgy, H.; Calzaferri, G.; Herren, D.; Zhdanov, A. *Chimia* **1991**, *45*, 3.
(6) Adrian, F. J. *J. Chem. Phys.* **1960**, *32*, 972.
(7) Dmitriev, Yu. A.; Zhitnikov, R. A. *Opt. Spektrosk.* **1990**, *69*, 1231.
(8) Spaeth, J.-M. *Hyperfine Interact.* **1996**, *32*, 641.
(9) Prassides, K.; Dennis, T. J. S.; Christides, C.; Roduner, E.; Kroto, H. W.; Taylor, R.; Walton, D. R. M. *J. Phys. Chem.* **1992**, *96*, 10600.
(10) Claxton, T. A. In *Protons and Muons in Materials Science*; Davis, E. A.; Cox, S. F. J., Eds.; Taylor & Francis Ltd.: London, Bristol, 1996.
(11) Roduner, E.; Percival, P. W.; Han, P.; Bartels, D. M. *J. Chem. Phys.* **1995**, *102*, 5989.
(12) Dilger, H.; Roduner, E.; Scheuermann, R.; Major, J.; Schefzik, M.; Stösser, R.; Päch, M.; Fleming, D. G. *Physica B* **2000**, *289*−*290*, 482.
(13) Petit, P.; Desainfuscien, M.; Audoin, C. *Metrologia* **1980**, *16*, 7.
(14) Wineland, D. J.; Ramsey, N. F. *Phys. Rev. A* **1972**, *5*, 821.
(15) *Cerius*^{2}, version 4.0; Molecular Simulations Inc.: San Diego, CA, 1999; http://www.msi.com.
(16) *MINUIT − Function Minimization and Error Analysis*, version 96.03; CERN Program Library Entry D506, Reference Manual; CERN: Geneva, Switzerland, 1996.
(17) Ramsey, N. F. *Molecular Beams*; Oxford University Press: New York, 1956.
(18) *MAPLE*, version 6.01; Waterloo Maple Inc.: Waterloo, Ontario, Canada, 2000; http://www.maplesoft.com.
(19) Auf der Heyde, T. P. E.; Bürgi, H.-B.; Bürgy, H.; Törnroos, K. W. *Chimia* **1991**, *45*, 38.
(20) Podberezskaya, N. V.; Magarill, S. A.; Baidina, I. A.; Borisov, S. V.; Gorsh, L. E.; Kanev, A. N.; Martynova, T. N. *J. Struct. Chem.* **1982**, *23*, 422.
(21) Engelhardt, G.; Zeigan, D.; Hoebbel, D.; Samoson, A.; Lippmaa, E. *Z. Chem.* **1982**, *22*, 314.
(22) Cambridge Structural Database. Cambridge Crystallographic Data Centre. http://www.ccdc.cam.ac.uk (2000).
(23) Weil, J. A.; Wertz, J. R.; Bolton, J. E. *Electron Paramagnetic Resonance*; John Wiley & Sons: New York, 1994.
(24) Bieniok, A. M.; Bürgi, H.-B. *J. Phys. Chem.* **1994**, *98*, 10735.
(25) Tiedeman, J. S.; Robinson, H. G. *Phys. Rev. Lett.* **1977**, *39*, 602.
(26) The NIST Reference on Constants, Units, and Uncertainity. National Institute of Standards and Technology. http://physics.nist.gov (2001).
(27) Atherton, N. M. *Principles of Electron Spin Resonance*; Ellis Horwood Ltd.: Chichester, U.K., 1993.
(28) Marcolli, C.; Lainé, P.; Bühler, R.; Calzaferri, G. *J. Phys. Chem. B* **1997**, *101*, 1171.